ORIGINAL RESEARCH

Decreasing the radiation dose for contrast-enhanced abdominal spectral CT with a half contrast dose: a matched-pair comparison with a 120 kVp protocol

[1,2]**DAISUKE SAKABE**, MS, [3]**TAKESHI NAKAURA**, MD, [3]**SEITARO ODA**, MD, [3]**MASAFUMI KIDOH**, MD,
[4]**DAISUKE UTSUNOMIYA**, MD, [2]**RT MASAHIRO HATEMURA** and [5]**YOSHINORI FUNAMA**, PhD

[1]Graduate School of Health Sciences, Kumamoto University, Kumamoto, Japan
[2]Department of Radiology, Kumamoto University Hospital, Kumamoto, Japan
[3]Department of Diagnostic Radiology, Faculty of Life Sciences, Kumamoto University, Kumamoto, Japan
[4]Diagnostic Radiology, Yokohama City University Graduate School of Medicine, Yokohama, Japan
[5]Department of Medical Physics, Faculty of Life Sciences, Kumamoto University, Kumamoto, Japan

Address correspondence to: Yoshinori Funama
E-mail: funama@kumamoto-u.ac.jp

Objectives: To compare the estimated radiation dose of 50% reduced iodine contrast medium (halfCM) for virtual monochromatic images (VMIs) with that of standard CM (stdCM) with a 120 kVp imaging protocol for contrast-enhanced CT (CECT).

Methods: We enrolled 30 adults with renal dysfunction who underwent abdominal CT with halfCM for spectral CT. As controls, 30 matched patients without renal dysfunction using stdCM were also enrolled. CT images were reconstructed with the VMIs at 55 keV with halfCM and 120 kVp images with stdCM and halfCM. The Monte-Carlo simulation tool was used to simulate the radiation dose. The organ doses were normalized to CTDIvol for the liver, pancreas, spleen, and kidneys and measured between halfCM and stdCM protocols.

Results: For the arterial phase, the mean organ doses normalized to CTDIvol for stdCM and halfCM were 1.22 and 1.29 for the liver, 1.50 and 1.35 for the spleen, 1.75 and 1.51 for the pancreas, and 1.89 and 1.53 for the kidneys. As compared with non-enhanced CT, the average increase in the organ dose was significantly lower for halfCM (13.8% ± 14.3 and 26.7% ± 16.7) than for stdCM (31.0% ± 14.3 and 38.5% ± 14.8) during the hepatic arterial and portal venous phases ($p < 0.01$).

Conclusion: As compared with stdCM with the 120 kVp imaging protocol, a 50% reduction in CM with VMIs with the 55 keV protocol allowed for a substantial reduction of the average organ dose of iodine CM while maintaining the iodine CT number for CECT.

Advances in knowledge: This study provides that the halfCM protocol for abdominal CT with a dual-layer-dual-energy CT can significantly reduce the increase in the average organ dose for non-enhanced CT as compared with the standard CM protocol.

INTRODUCTION

Recent technological advances have expanded the range of the clinical applications of multidetector CT. However, the widespread use of CT has raised concerns of the stochastic risk of radiation-induced cancer.[1–3] Generally, the effective dose (E) is estimated by multiplying the dose–length product (DLP) or CT dose index (CTDI) with standardized conversion factors as calculated using phantom-based Monte-Carlo simulation.[4,5] However, recent studies have suggested that the E/DLP and E/CTDI conversion factors for contrast-enhanced CT (CECT) are higher than those for non-enhanced CT (NECT) due to the photoelectric effect, and the use of a contrast medium (CM) can possibly increase the radiation dose by more than previously expected.[6–11] Such an increase in the radiation dose might

pose a severe problem for patients with abdominal malignant tumors who require frequent follow-up CECT.[12–15]

The findings of these previous reports suggest that the radiation dose can be reduced by reducing the CM dose. The most widely used method for CM dose reduction in CT might be low-kVp CT. However, it is uncertain whether this technique also decreases the E/DLP conversion factor because the photoelectric effect increases in low-kVp CT.[16] Recently, dual-layer dual-energy CT (DL-DECT) was introduced for clinical use.[17,18] DL-DECT can create virtual monochromatic images (VMIs) at different monochromatic X-ray energies (keV) under normal kVp settings (120 or 140 kVp). Previous reports have suggested that this system is useful to reduce the CM dose for abdominal

DL-DECT.[19] They concluded that DL-DECT at 40- to 55-keV provides equivalent or better image quality and lesion conspicuity for multiphasic-hepatic CT with 50% iodine-load without increasing radiation dose compared with standard 120-kVp protocol. Therefore, if the CM dose can be decreased for low-keV images using normal kVp settings, it is possible to decrease the radiation dose compared with that used in the standard CM (stdCM) protocol. To the best of our knowledge, this is the first study to compare the estimated radiation dose in a protocol involving low CM dose with DL-DECT compared with that used in the stdCM protocol.

The purpose of this study was to compare the estimated radiation dose between 50% reduced CM dose with the VMI protocol and stdCM with the 120-kVp protocol using DL-DECT.

Methods and materials
Study population
The protocol of this retrospective study was approved by the local institutional review board, which waived the requirement for informed consent.

The study cohort included 33 adults with renal dysfunction (estimated glomerular filtration rate <45 mL/min/1.73 m^2) who underwent abdominal CT with 50% reduced iodinated CM (halfCM) between December 2016 and June 2017. Among these patients, three were excluded from the study because the injection speed was reduced using a 24 G catheter. The remaining 30 patients were enrolled in this study. We also identified 341 adults who underwent CT with the stdCM protocol between April 2016 and June 2017. To reduce the potential confounding effects in this study, propensity score matching was performed using body weight, age, and sex of all patients (Figure 1). Finally, 30 patients for halfCM protocol and 30 patients for stdCM protocol were enrolled.[20,21] As shown in Table 1, there were no significant differences in terms of age, sex, or body weight between the groups.

Helical CT
All patients were examined with DL-DECT using the IQon Spectral CT system (Philips Healthcare, Cleveland, OH, USA). Two energy X-ray spectra were generated using a conventional single-tube voltage beam and dual-layer detectors. The single-tube

Figure 1. Flowchart of the patient enrollment process in this study.

Table 1. Patient characteristics

		StdCM	HalfCM	*p* value
		(*n* = 30)	(*n* = 30)	
Sex (male/female)		13/17	13/17	0.83a
Age (years)		69.5 ± 9.9	69.8 ± 11.5	0.93b
Body weight (kg)		54.0 ± 13.5	54.1 ± 13.2	0.98b

Data are presented as the mean ± standard deviation.
[a]Fisher's exact test
[b]Student's *t*-test

voltage for obtaining VMIs was set at 120 kVp. The scanning parameters for all image acquisitions were as follows: detector configuration, 64×0.625 mm (detector collimation); gantry rotation time, 0.5 s; and helical pitch (beam pitch), 0.8. Tube current modulation with automatic exposure control was set using an image quality reference [DoseRight Index (DRI); Philips Healthcare]. DRI was based on the relationship between the reference diameter and water equivalent diameter calculated based on the cross-sectional attenuation characteristic of patients. In this study, NECT and CECT during the hepatic arterial and portal venous phases (CECTa and CECTp, respectively) were achieved with a DRI of 22 to maintain constant image quality regardless of patient attenuation characteristics.

CM injection protocol
Regarding the stdCM protocol, 600 mgI/kg of CM (Omnipaque 300; Daiichi-Sankyo, Tokyo, Japan or Iomeron 300; Eisai Co., Ltd., Tokyo, Japan; or Iopamiron 370; Bayer Healthcare, Osaka, Japan) was delivered within 33.0 s followed by 30 ml of saline solution. CECTa and CECTp were started at 35 and 80 s after CM injection, respectively. We also delivered a 50% reduced iodinated CM dose of 300 mgI/kg in the halfCM protocol within 33.0 s followed by 30 ml of saline solution. CECTa and CECTp were started at 37 and 80 s after CM injection, respectively. Regarding CECTa, the scan start time for the halfCM protocol was 2.0 s later than that for the stdCM protocol due to the slower half injection rate.

CT image reconstruction
CT images were reconstructed with 120-kVp images using stdCM and halfCM protocols on NECT. With respect to CECT, CT images were reconstructed with 120-kVp images acquired using stdCM and halfCM protocols as well as 55-keV VMIs acquired using the halfCM protocol. In our previous study, the image noise and contrast-to-noise ratio with 55-keV images were close to the values compared with 120-kVp images. All images were acquired at a slice thicknesses of 5.0 mm and slice interval of 5.0 mm with an abdominal standard kernel (C) in a 30–35 cm display field of view depending on a patient's body size. In addition, denoizing level 3 (iDose^4 level 3; Philips Healthcare) was applied to the 120-kVp images and 55-keV VMIs to reduce image noise.

CT number based on organs
A board-certified radiologist with 22-year abdominal CT experience performed all quantitative image analyses of NECT, CTCTa,
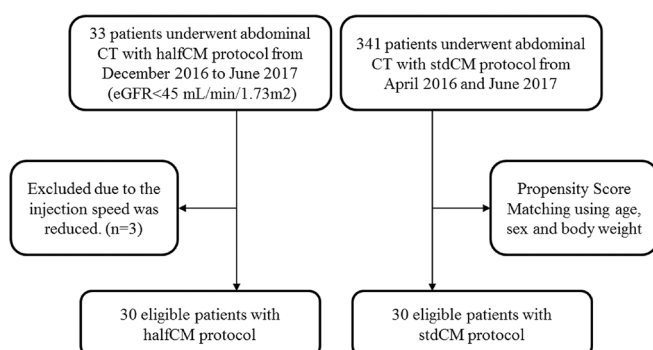
Figure 2. ROI placement for CT number and organ dose measurements in the liver (a), pancreas (b), spleen (c), and right and left kidneys (d) on CECT images.

and CECTp images. The CT numbers for the liver, pancreas, spleen, and both kidneys of each patient were measured using 120-kVp and 55-keV images acquired on NECT, CECTa, and CECTp, and the mean values were calculated. The region of interest (ROI) was positioned in the healthy parenchyma at the middle level of each organ to avoid vessels and to delineate the region where CM was homogeneously distributed (Figure 2). The CT numbers for the liver were measured in the right lobes, whereas those of both kidneys were measured at the level of the renal hilum. ROIs identical in terms of size, shape, and anatomical position were employed for NECT and the corresponding CECT images of the same patient.

Organ dose estimation

The Monte-Carlo simulation tool (ImpactMC; VAMP GmbH, Erlangen, Germany) was used to simulate the radiation dose delivered to each patient for NECT and CECT. For the X-ray spectrum data, shaped filters were used for the Monte-Carlo simulation of the actual measurement values of the half-value layer of aluminum and the off-center ratio as described previously.[22,23] The tube current modulation from the top-to-bottom slice levels of each patient was also included in the Monte-Carlo simulation.[24] The individual organ doses for the liver, pancreas, spleen, and both kidneys for each patient were acquired from the values acquired on Monte-Carlo simulation. With the Monte-Carlo simulation, air, water, and bone materials were used for NECT. Regarding CECT, the Monte-Carlo simulation included iodinated CM and its relationship with iodine enhancement in images because the iodine volume increased with increasing iodine enhancement, and volume fraction was different between the 55-keV and 120-kVp images. For organ-dose measurements, the same ROIs as used for CT number measurements (size, shape, and anatomical position) were employed for NECT and CECT images of the same patient. The volume CTDI (CTDIvol) was recorded in milligray units for all images, and the measured organ doses were normalized to the corresponding CTDIvol at the same slice level to correct the difference in dose from the

original dose. In addition, the increase in the organ dose caused by iodinated CM was calculated as follows:

% organ dose increase = (organ dose/CTDIvol) CECT

(organ dose/CTDIvol) NECT)/(organ dose/CTDIvol) NECT100(%)

Statistical analysis

All quantitative images acquired with the stdCM and halfCM protocols were compared. Differences in the mean CT numbers among the three types of images were determined with Dunnett's test, using the values acquired from the 120-kVp images acquired using the stdCM protocol as a control. The Welch's t-test was used to compare the organ dose between the stdCM and halfCM protocols. A probability (p) value of <0.05 was considered statistically significant. All statistical analyses were performed with R v.3.5.1 (The R project for statistical computing; http://www.r-project.org/).

RESULTS

CT numbers for 120-kVp and 55-keV images

Regarding CECTa, the mean CT numbers for the 120-kVp images acquired with the stdCM protocol, 55-keV images acquired with the halfCM protocol, and 120-kVp images acquired with the halfCM protocol were 73 ± 10.2, 72 ± 17.2, and 65 ± 11.0 Hounsfield unit (HU) for the liver; 103 ± 29.3, 96 ± 23.0, and 68.0 ± 21.2 HU for the pancreas; 141 ± 26.1, 118 ± 25.0, and 90 ± 14.7 HU for the spleen; and 139 ± 24.7, 134 ± 42.7, and 79 ± 19.6 HU for the kidneys, respectively. Further, for all organs, the mean CT numbers for the 55-keV images acquired with the halfCM protocol were significantly higher than those for the 120-kVp images acquired with the halfCM protocol, but they were equivalent to the 120-kVp images acquired with the stdCM protocol(Table 2).

Figure 3 shows the increase in the mean CT numbers from NECT to CECTa and CECTp. Concerning CECTa (Figure 3a) and CECTp (Figure 3b), the increases in the mean CT numbers for the 55-keV images acquired with the halfCM protocol were equivalent to those for the 120-kVp images acquired with the stdCM protocol, except for the spleen by CECTa ($p > 0.05$).

Figure 3. Increase in the mean CT number for 120-kVp images acquired using standard CM (StdCM), 55-keV images acquired using 50% CM dose (halfCM), and 120-kVp images acquired using halfCM from NECT to CECT during hepatic arterial phase (a) and portal venous phase (b).
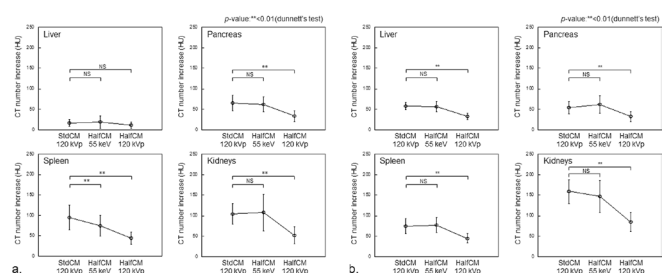
Table 2. Organ CT number for 120 kVp and 55 keV images with standard CM and halfCM

Organ	NECT		CECTa			CECTp		
	StdCM	HalfCM	StdCM	HalfCM		StdCM	HalfCM	
	120 kVp	120 kVp	120 kVp	55 keV	120 kVp	120 kVp	55 keV	120 kVp
Liver	56 ± 5.9	54 ± 8.7	73 ± 10.2	72 ± 17.2	65 ± 11	114 ± 9.7	109 ± 14.5	87 ± 12.3
Pancreas	37 ± 17.4	34 ± 17.1	103 ± 29.3	96 ± 23	68 ± 21.2	91 ± 22.5	95 ± 18.2	67 ± 18.5
Spleen	47 ± 3.7	46 ± 4.5	141 ± 26.1	118 ± 25	90 ± 14.7	121 ± 12.3	121 ± 17.7	90 ± 10.5
Kidneys	35 ± 4.7	31 ± 2.9	139 ± 24.7	134 ± 42.7	79 ± 19.6	194 ± 28.4	172 ± 35.8	112 ± 22.4

Effect of organ dose between stdCM and halfCM

The mean organ doses for NECT, CECTa, and CECTp are presented in Table 3. For CECTa, the halfCM organ dose was equivalent to or lower than that for stdCM, and there were significant differences in the organ dose delivered to the pancreas, spleen, and kidneys (pancreas: $p < 0.01$, 18.9 ± 3.5 vs. 22.0 ± 3.5 mGy; spleen: $p < 0.01$, 21.5 ± 4.4 mGy and 26.0 ± 4.3 mGy; and kidneys: $p < 0.01$, 20.4 ± 4.6 mGy and 26.5 ± 4.6 mGy). With respect to the kidneys imaged using CECTp, the halfCM organ dose was also lower than the stdCM organ dose ($p < 0.01$, 24.5 ± 5.8 vs. 32.9 ± 4.7 mGy).

Table 4 shows the percentage of organ dose increase from NECT to CECT due to the iodinated CM effect. The organ dose increased from NECT to CECTa, and the mean increase of stdCM *vs* halfCM was 26.3±15.0% *vs* 11.2%±12.9% for the pancreas, 46.1±18.6% *vs* 24.1%±17.6% for the spleen, and 43.2±17.1% *vs* 12.4%±18.1% for the kidneys, respectively, (all $p < 0.01$). The percentage increase in the halfCM value was lower than that in the stdCM value. With respect to the liver, the organ dose increase was 8.5±6.6% with the stdCM protocol and 7.6±8.7% with the halfCM protocol without any significant difference ($p > 0.05$). Compared with NECT, the mean increase in the organ dose was significantly lower for the halfCM protocol (13.8±14.3%) than for the stdCM protocol (31.0±14.3%) in CECTa ($p < 0.01$) (Figure 4a).

Regarding CECTp, the highest mean increase in the organ dose for the stdCM protocol was acquired at 79.9±22.2% for the kidneys (halfCM: 36.7±21.1%, $p < 0.01$). The other organ doses for stdCM *vs* halfCM protocols also increased by 20.4±8.6% *vs* 21.7%±14.0% for the liver, 19.9±12.7% *vs* 14.2%±14.0% for the pancreas, and 33.6±15.7% and 34.3±17.8% for the spleen. However, there was no significant difference between stdCM and halfCM protocols in this regard ($p > 0.05$). Compared with NECT, the mean increase in the organ dose was significantly lower for the halfCM protocol (26.7±16.7%) than for the stdCM protocol (38.5±14.8%) with CECTp ($p < 0.01$, Figure 4b). The representative CT images and dose distributions for stdCM and halfCM protocols are shown in Figure 5.

DISCUSSION

In this study, we compared the estimated radiation dose between 50% reduced CM dose with the VMI protocol and stdCM with

Figure 4. Increase in the mean organ dose for NECT to CECT during hepatic arterial phase (a) and portal venous phase (b) due to the iodinated CM effect.
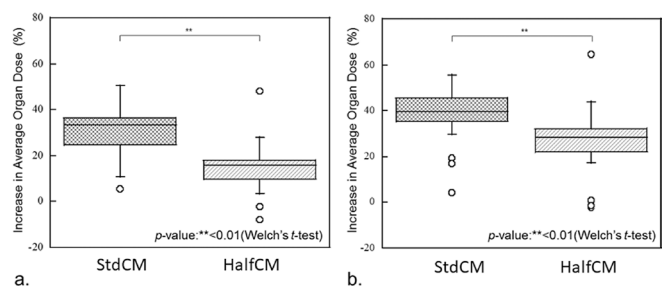
Table 3. Mean organ dose for NECT and CECT

Organ	Organ dose (mGy)											
	NECT				CECTa				CECTp			
	StdCM		HalfCM		StdCM		HalfCM		StdCM		HalfCM	
Liver	13.3 ±	2.1	13.4 ±	2.4	18.0 ±	2.5	17.9 ±	3.2	19.8 ±	2.7	19.9 ±	3.5
Pancreas	13.9 ±	1.9	13.8 ±	2.2	22.0 ±	3.5	18.9** ±	3.5	20.7 ±	2.9	19.2 ±	3.8
Spleen	14.4 ±	2.3	14.0 ±	2.8	26.0 ±	4.3	21.5** ±	4.4	23.9 ±	4.8	22.8 ±	4.3
Kidneys	14.9 ±	3.0	15.0 ±	4.1	26.5 ±	4.6	20.4** ±	4.6	32.9 ±	4.7	24.5** ±	5.8

p-value: ** <0.01 (Welch's t-test)

NECT: non-enhanced CT
CECTa: contrast-enhanced CT during the hepatic arterial phase
CECTp: contrast-enhanced CT during the portal venous phase
StdCM: standard contrast medium protocol
HalfCM: half contrast medium protocol
Data are presented as the mean ± standard deviation.

Figure 5. CT images and dose distributions acquired for the standard CM and 50% CM dose protocols during hepatic arterial and portal venous phases. A 74-year-old female (body weight, 44.0 kg) received standard CM for the hepatic arterial phase (a,c) and the portal venous phase (b,d). A 73-year-old female (body weight, 44.0 kg) received 50% CM dose for the hepatic arterial phase (e,g) and portal venous phase (f, h). The CT images acquired at 120 kVp (a,b) and VMI acquired at 55 keV (e,f).
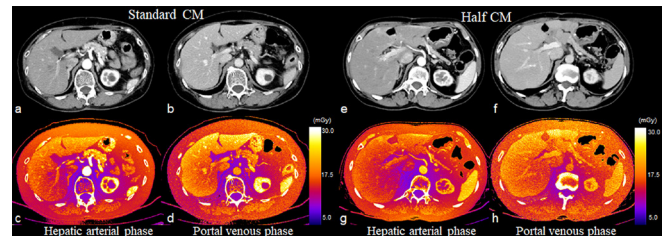
the 120-kVp protocol using DL-DECT. For CECTa and CECTp, the halfCM organ dose was equivalent to or lower than that for stdCM. Besides, compared with NECT, the increase in the organ dose was significantly lower for the halfCM protocol than for the stdCM protocol in CECTa and CECTp. The rate of radiation dose reduction widely varied among the studied organs. The results of the present study suggested that the halfCM protocol for abdominal DL-DECT can significantly reduce the increase in the mean organ dose for NECT compared with the stdCM protocol.

To the best of our knowledge, this is the first report to evaluate whether a CM dose reduction in CT can also decrease the radiation dose. Previous reports have suggested that the increase in the CT number by CM is mainly caused by the photoelectric effect, which can also increase the radiation dose.[6–11] Concerning CECT, previous reports have suggested that the organ dose increased by the use of iodinated CM because of its high atomic number. A high concentration of CM not only proportionally increases the effective atomic number of objects and results in a high CT number but also increases the ionizing radiation, which results in an increase in the organ dose. Because the CM dose reduction protocol decreases the concentration of CM in organs, it can also possibly decrease absorption via the photoelectric effect. These results suggest that CM dose reduction in abdominal CT also reduced the increase in the mean organ dose in NECT.

Another important finding of this study is that the radiation dose reduction by the halfCM protocol widely varied among the studied organs. The radiation dose reduction rate was high in the kidneys, but it was extremely low in the pancreas and liver. The iodine concentration in the kidneys is generally higher than that in the pancreas and liver. Therefore, it is reasonable that the CM dose reduction might be effective to reduce the radiation dose, particularly in the kidneys. However, the organ doses of the pancreas and liver were nearly not reduced by CM dose reduction. Although we cannot explain the detailed mechanisms underlying this phenomenon, the iodine concentration and anatomical sites of the organs may be responsible for these results. The iodine concentration in the liver was relatively low, which might result in a reduction in the CM dose compared with

Table 4. Increase in the organ dose of NECT to CECT due to the iodine CM effect

Organ	Percentage of organ dose increase (%)										
	CECTa						CECTp				
	StdCM			HalfCM			StdCM			HalfCM		
Liver	8.5	±	6.6	7.6	±	8.7	20.4	±	8.6	21.7	±	14.0
Pancreas	26.3	±	15.0	11.2**	±	12.9	19.9	±	12.7	14.2	±	14.0
Spleen	46.1	±	18.6	24.1**	±	17.6	33.6	±	15.7	34.3	±	17.8
Kidneys	43.2	±	17.1	12.4**	±	18.1	79.9	±	22.2	36.7**	±	21.1
Average	31.0	±	14.3	13.8**	±	14.3	38.5	±	14.8	26.7**	±	16.7

p-value: **<0.01(Welch's t-test)
NECT: non-enhanced CT
CECTa: contrast-enhanced CT during the hepatic arterial phase
CECTp: contrast-enhanced CT during the portal venous phase
StdCM: standard contrast medium protocol
HalfCM: half contrast medium protocol
Data are presented as the mean ± standard deviation.

those in the kidneys and pancreas. On the other hand, the iodine concentration in the pancreas was relatively high compared with that in the liver. However, the halfCM protocol did not reduce the radiation dose related to the pancreas in this study. We believe that the long distance from the skin to pancreas resulted in this phenomenon. The halfCM protocol decreased X-ray absorption from the skin to pancreas and increased X-ray transmission to the pancreas. Therefore, we believe that the increased X-ray transmission compensates for the decreased photoelectric effect in the pancreas by the halfCM protocol.

It is uncertain whether the halfCM protocol always decreases the radiation dose. DL-DECT separates the X-ray beam into high- and low-energy datasets with the use of a single X-ray tube (120 or 140 kVp) and dual-layer detector. Therefore, we can use highly iodinated CM of a lower keV setting without the need for a change in the X-ray tube setting to reduce the CM dose in this study. On the other hand, other DECT systems use high- and low-tube voltage scans to obtain two energy datasets. However, further studies are needed to determine whether the iodinated CM reduction protocol with low-tube voltage or other DECT systems can also decrease the radiation dose because a low-kVp CT also increases the photoelectric effect.

Unlike the other organs, the increase in the mean CT numbers from NECT to CECTa for the liver at photon energy of 120 kVp with the halfCM protocol was almost equivalent to that at 120 kVp with the stdCM protocol (11 *vs* 17 HU, respectively) because the hepatic arterial phase is the optimal scan timing for the detection of hepatocellular carcinoma and normal CM enhancement for normal liver parenchyma is acquired during the portal venous phase.

There were some limitations to this study. First, the center position of the liver was used for measurements. Measurement of the radiation doses inside or outside of the liver portions might have a different effect on radiation dose reduction. Next, we compared the effect of the organ dose between stdCM and halfCM to obtain the same CT numbers of the organs. Furthermore, settings with a lower keV might contribute to reductions in CM and organ doses. Finally, the number of patients was relatively small. Thus, further large-scale studies will be needed to validate our results.

CONCLUSION
Compared with stdCM with the 120-kVp imaging protocol, 50% reduced CM with VMI with the 55-keV protocol allowed for a substantial reduction in the increase in the mean organ dose of iodinated CM while maintaining the iodinated CT number for CECT.

REFERENCES

1. Brenner DJ, Hall EJ. Computed tomography--an increasing source of radiation exposure. *N Engl J Med* 2007; **357**: 2277–84. doi: https://doi.org/10.1056/NEJMra072149

2. Sodickson A, Baeyens PF, Andriole KP, Prevedello LM, Nawfel RD, Hanson R, et al. Recurrent CT, cumulative radiation exposure, and associated radiation-induced cancer risks from CT of adults. *Radiology* 2009; **251**: 175–84. doi: https://doi.org/10.1148/radiol.2511081296

3. Berrington de González A, Darby S. Risk of cancer from diagnostic X-rays: estimates for the UK and 14 other countries. *Lancet* 2004; **363**: 345–51. doi: https://doi.org/10.1016/S0140-6736(04)15433-0

4. Christner JA, Kofler JM, McCollough CH. Estimating effective dose for CT using dose-length product compared with using organ doses: consequences of adopting international Commission on radiological protection publication 103 or dual-energy scanning. *AJR Am J Roentgenol* 2010; **194**:

881–9. doi: https://doi.org/10.2214/AJR.09.3462

5. Deak PD, Smal Y, Kalender WA. Multisection CT protocols: sex- and age-specific conversion factors used to determine effective dose from dose-length product. *Radiology* 2010; **257**: 158–66. doi: https://doi.org/10.1148/radiol.10100047

6. Amato E, Lizio D, Settineri N, Di Pasquale A, Salamone I, Pandolfo I. A method to evaluate the dose increase in CT with iodinated contrast medium. *Med Phys* 2010; **37**: 4249–56. doi: https://doi.org/10.1118/1.3460797

7. Amato E, Salamone I, Naso S, Bottari A, Gaeta M, Blandino A. Can contrast media increase organ doses in CT examinations? a clinical study. *AJR Am J Roentgenol* 2013; **200**: 1288–93. doi: https://doi.org/10.2214/AJR.12.8958

8. Sahbaee P, Segars WP, Marin D, Nelson RC, Samei E. The effect of contrast material on radiation dose at CT: Part I. incorporation of contrast material dynamics in Anthropomorphic phantoms. *Radiology* 2017; **283**: 739–48. doi: https://doi.org/10.1148/radiol.2016152851

9. Sahbaee P, Abadi E, Segars WP, Marin D, Nelson RC, Samei E. The effect of contrast material on radiation dose at CT: Part II. A systematic evaluation across 58 patient models. *Radiology* 2017; **283**: 749–57. doi: https://doi.org/10.1148/radiol.2017152852

10. Paul J, Schell B, Kerl JM, Maentele W, Vogl TJ, Bauer RW. Effect of contrast material on image noise and radiation dose in adult chest computed tomography using automatic exposure control: a comparative study between 16-, 64- and 128-slice CT. *Eur J Radiol* 2011; **79**: e128–32. doi: https://doi.org/10.1016/j.ejrad.2011.05.012

11. Perisinakis K, Tzedakis A, Spanakis K, Papadakis AE, Hatzidakis A, Damilakis J. The effect of iodine uptake on radiation dose absorbed by patient tissues in contrast enhanced CT imaging: implications for CT dosimetry. *Eur Radiol* 2018; **28**: 151–8. doi: https://doi.org/10.1007/s00330-017-4970-1

12. Ronot M, Vilgrain V. Hepatocellular carcinoma: diagnostic criteria by imaging techniques. *Best Pract Res Clin Gastroenterol* 2014; **28**: 795–812. doi: https://doi.org/10.1016/j.bpg.2014.08.005

13. Iwakiri Y, Shah V, Rockey DC. Vascular pathobiology in chronic liver disease and cirrhosis - current status and future directions. *J Hepatol* 2014; **61**: 912–24. doi: https://doi.org/10.1016/j.jhep.2014.05.047

14. Sandrasegaran K, Maglinte DDT, Howard TJ, Kelvin FM, Lappas JC. The multifaceted role of radiology in small bowel obstruction. *Semin Ultrasound CT MR* 2003; **24**: 319–35. doi: https://doi.org/10.1016/S0887-2171(03)00072-6

15. Tang ZH, Qiang JW, Feng XY, Li RK, Sun RX, Ye XG, RK L, XG Y. Acute mesenteric ischemia induced by ligation of porcine superior mesenteric vein: multidetector CT evaluations. *Acad Radiol* 2010; **17**: 1146–52. doi: https://doi.org/10.1016/j.acra.2010.04.014

16. Huda W, Ogden KM, Khorasani MR. Converting dose-length product to effective dose at CT. *Radiology* 2008; **248**: 995–1003. doi: https://doi.org/10.1148/radiol.2483071964

17. Hickethier T, Baeßler B, Kroeger JR, Doerner J, Pahn G, Maintz D, et al. Monoenergetic reconstructions for imaging of coronary artery stents using spectral detector CT: in-vitro experience and comparison to conventional images. *J Cardiovasc Comput Tomogr* 2017; **11**: 33–9. doi: https://doi.org/10.1016/j.jcct.2016.12.005

18. van Hamersvelt RW, Schilham AMR, Engelke K, den Harder AM, de Keizer B, Verhaar HJ, et al. Accuracy of bone mineral density quantification using dual-layer spectral detector CT: a phantom study. *Eur Radiol* 2017; **27**: 4351–9. doi: https://doi.org/10.1007/s00330-017-4801-4

19. Nagayama Y, Nakaura T, Oda S, Utsunomiya D, Funama Y, Iyama Y, et al. Dual-layer DECT for multiphasic hepatic CT with 50 percent iodine load: a matched-pair comparison with a 120 kVp protocol. *Eur Radiol* 2018; **28**: 1719–30. doi: https://doi.org/10.1007/s00330-017-5114-3

20. McDonald JS, McDonald RJ, Carter RE, Katzberg RW, Kallmes DF, Williamson EE. Risk of intravenous contrast material-mediated acute kidney injury: a propensity score-matched study stratified by baseline-estimated glomerular filtration rate. *Radiology* 2014; **271**: 65–73. doi: https://doi.org/10.1148/radiol.13130775

21. Nagayama Y, Tanoue S, Tsuji A, Urata J, Furusawa M, Oda S, et al. Application of 80-kVp scan and raw data-based iterative reconstruction for reduced iodine load abdominal-pelvic CT in patients at risk of contrast-induced nephropathy referred for oncological assessment: effects on radiation dose, image quality and renal function. *Br J Radiol* 2018; **91**: 20170632. doi: https://doi.org/10.1259/bjr.20170632

22. Tucker DM, Barnes GT, Chakraborty DP. Semiempirical model for generating tungsten target X-ray spectra. *Med Phys* 1991; **18**: 211–8. doi: https://doi.org/10.1118/1.596709

23. McKenney SE, Nosratieh A, Gelskey D, Yang K, Huang S-Y, Chen L, et al. Experimental validation of a method characterizing bow tie filters in CT scanners using a real-time dose probe. *Med Phys* 2011; **38**: 1406–15. doi: https://doi.org/10.1118/1.3551990

24. Kalender WA, Wolf H, Suess C. Dose reduction in CT by anatomically adapted tube current modulation. II. phantom measurements. *Med Phys* 1999; **26**: 2248–53. doi: https://doi.org/10.1118/1.598738